AD-A160 887 INVESTIGATE LASER INDUCED DAMAGE IN OPTICAL COATINGS USING TIME RESOLVED..(U) BATTELLE MEMORIAL INST RICHLAND WASH PACIFIC NORTHWEST LABS G J EXARHOS 1/1

UNCLASSIFIED AUG 85 AFWL-TN-84-72 F/G 20/6 NL

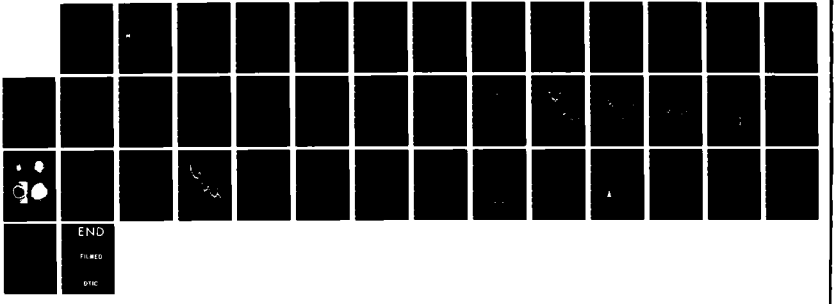

END

FILMED

DTIC

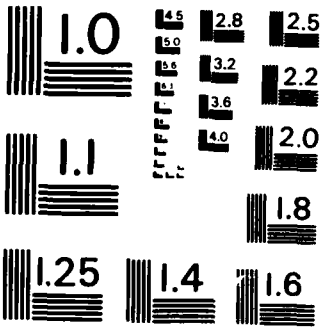

AFWL-TN-84-72

(2)

INVESTIGATE LASER INDUCED DAMAGE IN OPTICAL COATINGS USING TIME RESOLVED RAMAN SPECTROSCOPY

Gregory J. Exarhos

Pacific Northwest Laboratory
Richland, Washington 99352

August 1985

Final Report

AIR FORCE WEAPONS LABORATORY
Air Force Systems Command
Kirtland Air Force Base, NM 87117-6008

This final report was prepared by Pacific Northwest Laboratory, Richland, Washington under Purchase Order 84-044, Job Order ILIR8403 with the Air Force Weapons Laboratory, Kirtland Air Force Base, New Mexico. Capt Patricia L. Morse (ARBE) was the Laboratory Project Officer-in-Charge.

When Government drawings, specifications or other data are used for any purpose other than in connection with a definitely Government-related procurement, the United States Government incurs no responsibility or any obligation whatsoever. The fact that the Government may have formulated or in any way supplied the said drawings, specifications or other data is not to be regarded by implication, or otherwise in any manner construed, as licensing the holder, or any other person or corporation; or as conveying any rights or permission to manufacture, use or sell any patented invention that may in any way be related thereto.

This report has been reviewed by the Public Affairs Office and is releasable to the National Technical Information Services (NTIS). At NTIS, it will be available to the general public, including foreign nations.

This report has been authored by a contractor of the United States Government. Accordingly, the United States Government retains a nonexclusive, royalty-free license to publish or reproduce the material contained herein, or allow others to do so, for the United States Government purposes.

If your address has changed, if you wish to be removed from our mailing list, or if your organization no longer employs the addressee, please notify AFWL/ARBE, Kirtland AFB, NM 87117-6008 to help us maintain a current mailing list.

Patricia L. Morse

PATRICIA L. MORSE
Capt, USAF
Project Officer

FOR THE COMMANDER

William J. Welker Jr

WILLIAM J. WELKER, JR.
Capt, USAF
Chief, Optical Components Branch

William T. Guenther

DR ARTHUR GUENTHER
Chief Scientist

DO NOT RETURN COPIES OF THIS REPORT UNLESS CONTRACTUAL OBLIGATIONS OR NOTICE ON A SPECIFIC DOCUMENT REQUIRES THAT IT BE RETURNED.

UNCLASSIFIED

SECURITY CLASSIFICATION OF THIS PAGE

AD-A160887

REPORT DOCUMENTATION PAGE

1a. REPORT SECURITY CLASSIFICATION UNCLASSIFIED	1b. RESTRICTIVE MARKINGS
2a. SECURITY CLASSIFICATION AUTHORITY	3. DISTRIBUTION/AVAILABILITY OF REPORT Approved for public release; distribution unlimited.
2b. DECLASSIFICATION/DOWNGRADING SCHEDULE	
4. PERFORMING ORGANIZATION REPORT NUMBER(S)	5. MONITORING ORGANIZATION REPORT NUMBER(S) AFWL-TN-84-72
6a. NAME OF PERFORMING ORGANIZATION Pacific Northwest Laboratory 6b. OFFICE SYMBOL (If applicable)	7a. NAME OF MONITORING ORGANIZATION Air Force Weapons Laboratory
6c. ADDRESS (City, State and ZIP Code) Richland, Washington 99352	7b. ADDRESS (City, State and ZIP Code) Kirtland Air Force Base, NM 87117-6008
8a. NAME OF FUNDING/SPONSORING ORGANIZATION 8b. OFFICE SYMBOL (If applicable)	9. PROCUREMENT INSTRUMENT IDENTIFICATION NUMBER 84-044
8c. ADDRESS (City, State and ZIP Code)	10. SOURCE OF FUNDING NOS. PROGRAM ELEMENT NO.: 61101F; PROJECT NO.: ILIR; TASK NO.: 84; WORK UNIT NO.: 03
11. TITLE (Include Security Classification) INVESTIGATE LASER INDUCED DAMAGE IN OPTICAL COATINGS USING TIME RESOLVED RAMAN SPECTROSCOPY	
12. PERSONAL AUTHOR(S) Gregory J. Exarhos	
13a. TYPE OF REPORT Final 13b. TIME COVERED FROM Jan 84 TO Nov 84	14. DATE OF REPORT (Yr., Mo., Day) 1985, August 15. PAGE COUNT 44
16. SUPPLEMENTARY NOTATION	

17. COSATI CODES		
FIELD	GROUP	SUB. GR.
20	05	
11	03	

18. SUBJECT TERMS (Continue on reverse if necessary and identify by block number)
Laser Damage Mechanisms, Laser Heating, Time Resolved Raman Spectroscopy, Phase Transformations, Molecular Vibrational Studies, TiO_2 Optical Coatings

19. ABSTRACT (Continue on reverse if necessary and identify by block number)

Raman spectroscopy is shown to be a viable and rapid technique for characterization of laser induced damage in thin dielectric coatings on fused silica substrates. Unequivocal identification of crystalline and amorphous phases can be discerned from measured vibrational spectra. A two laser (damage-probe) technique has been developed for in situ analysis of laser damage to optical coatings. Raman measurements made at long times following pulsed laser damage serve to characterize the equilibrium damage state and can be used to spatially profile the damage zone. Time resolved measurements acquired within nanoseconds following the high energy laser pulse probe the transient response of the system. The dynamics of laser induced damage to optical coatings are studied by these and related Raman experiments from which mechanistic information can also be inferred. The primary mechanism of failure in titanium dioxide (TiO_2) coatings results from crystalline phase changes induced thermally or by multiphoton excitation processes. A similar failure mode is predicted for other oxidic coatings such as zirconium dioxide (ZrO_2) which can exist in different room temperature stable phases.

20. DISTRIBUTION/AVAILABILITY OF ABSTRACT UNCLASSIFIED/UNLIMITED ☒ SAME AS RPT. ☐ DTIC USERS ☐	21. ABSTRACT SECURITY CLASSIFICATION UNCLASSIFIED
22a. NAME OF RESPONSIBLE INDIVIDUAL Capt Patricia L. Morse	22b. TELEPHONE NUMBER (Include Area Code) (505) 844-1776 22c. OFFICE SYMBOL ARBE

DD FORM 1473, 83 APR EDITION OF 1 JAN 73 IS OBSOLETE.

UNCLASSIFIED

SECURITY CLASSIFICATION OF THIS PAGE

SUMMARY

This report describes a pioneering application of laser Raman spectroscopy to real time characterization of pulsed laser damage to optical coatings. Since Raman scattering results from an electromagnetic interaction with molecular vibrations, this technique is a direct probe of localized chemical bonding and provides bond strength as well as localized structural information. Recent advances in detector sensitivity and increased fast gating capability enable full Raman spectra excited by a single probe laser pulse to be acquired on a nanosecond time scale. The in situ capability of Raman spectroscopy makes it an attractive technique, for probing chemical bonding changes during and following high energy pulsed laser damage to optical coatings.

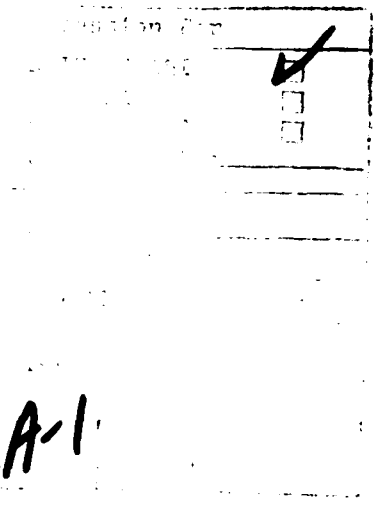

A-1

CONTENTS

ILLUSTRATIONS

ILLUSTRATIONS (Contd)

1.0 INTRODUCTION

The feasibility of using in situ Raman spectroscopy to characterize high energy pulsed laser induced surface damage in dielectric optical coatings has been demonstrated by this nondestructive inelastic light scattering technique. Energy differences between incident and scattered photons correspond to allowed vibrational transitions of the material under investigation. The number of observed vibrational transitions can structurally identify a particular material or phase while band frequency shifts correlate with chemical bond length or bond angle changes induced by temperature or pressure effects (Refs. 1 and 2). Raman optical measurements can provide, in theory, more extensive microstructural information than the reflection or transmission measurements commonly used to indicate the onset of damage during laser irradiation testing of dielectric mirrors. Raman information is used to deduce a mechanistic interpretation of the damage process which will aid in the development of new coatings having higher optimized damage thresholds.

The interaction of high energy laser irradiation with dielectric surfaces which eventually results in catastrophic damage involves a number of energy transfer/relaxation processes as detailed in Figure 1. Rapid energy transfer from a high energy laser pulse to an optical coating can lead to structural changes within the thin film resulting from electronic excitation and localized heating. Surface decomposition, melting, and recrystallization can then result. Each of these physical transformations is accompanied by marked changes in localized chemical bonding on a time-scale readily accessible to state-of-the-art Raman measurements. Therefore, in situ experiments have been conducted to probe chemical bonding changes in dielectric coatings that have been subjected to intense pulsed laser irradiation.

Application of Raman spectroscopy to characterization of thin optical coatings has only recently been explored. Conventional measurements of single layer TiO_2 on silica have unequivocally identified the anatase phase in submicron sputter deposited coatings and demonstrated a linear correlation of bank intensities with thickness from 0.1 μm up to several micrometers (Ref. 3). The technique of interference enhancement has also been developed allowing Raman spectra of extremely thin films to be measured (Ref. 4 and 5). High quality spectra have also been acquired from all-dielectric multilayer

SiO_2/TiO_2 coatings of general or arbitrary design with no special specimen preparation required (Ref. 6). The Raman technique is also a sensitive probe of microcrystallite grain orientation in sputtered coatings through polarization analysis of the scattered light. Furthermore, suppression of substrate Raman scattering from coatings consisting of unoriented grains can be achieved through measurements of the appropriate polarization component of the scattered light enabling extremely thin coatings to be characterized by this technique (Ref. 7).

In this investigation, all coatings evaluated were deposited onto fused silica (SiO_2) substrates. For thinner coatings, the weak substrate Raman scattering can be appreciable relative to scattering from the thin film and can obscure Raman lines attributed to the coating. To minimize this substrate interference, a technique has been employed which takes advantage of the contrasting polarization properties of Raman scattering from the fused silica substrate and the fine grained coating. Inherent molecular disorder present in the fused silica results in marked polarization anisotropy in the Raman scattered radiation while scattering from the individual randomly orientated grains is isotropic. Therefore, analysis of the perpendicular component of the scattered light will consist almost entirely of Raman scattering attributed to the optical coatings. This effect is illustrated dramatically for thin TiO_2 coatings on silica in Figs. 2, 3 and 4.

Raman spectroscopy has been used to evaluate laser damage to single layer TiO_2 coatings on silica and more extensive measurements on multilayer coatings are currently in progress. Conventional measurements are used to characterize the equilibrium damage state where two colinear laser beams are directed at normal incidence to the sample under investigation. (A low energy continuous wave visible laser serves as the Raman probe while a high energy pulsed laser causes damage to the coatings.) Raman spectra measured before and after the damage pulse provide information on the survivability of the coating and substrate with respect to induced phase transformation and coating decomposition.

A second experiment has been designed to evaluate equilibrium damage in TiO_2 optical coatings caused by changes in sample temperature. Raman spectra are acquired while the sample is heated by an auxiliary CO_2 laser from room temperature to ca 1500°C. Under these conditions the sample is in thermal

equilibrium and the vibrational levels are populated according to the Boltzmann distribution. The Raman experiment probes the ground electronic state. Equilibrium phase transitions (anatase-rutile), should they occur, will be manifested in measured Raman spectra.

To study the dynamics of laser induced damage in optical coatings, time resolved Raman spectroscopy (TRRS) was used. Spectra were acquired at various delay times following the damage pulse. Under these nonequilibrium conditions the Raman experiment probes the excited electronic states of the material. Resonance enhancement of vibrational lines is possible leading to increased intensity of selective Raman modes. Interpretation of measured spectra can yield information concerning structure of the excited state.

The primary candidate coating material chosen for this project is TiO_2 deposited on silica substrates in both single layer and multilayer designs although some preliminary data from studies of ZrO_2 will also be discussed. These oxides were chosen for investigation not only because they are technologically important, but because they exhibit relatively high Raman scattering cross sections and can exist in several stable crystalline phases that are readily discernible from measured Raman spectra (Figs. 3 and 4).

Structures of the anatase and rutile phases of TiO_2 are shown in Figure 5. Titanium is localized in a nearly octahedral environment for both crystalline modifications, although TiO_2 distances for the lower density anatase phase are somewhat larger and the planar oxygen atoms assume a more puckered (tetrahedral) arrangement. Since rutile is the more thermodynamically stable phase (Ref. 8), a thermally induced irreversible phase transition is expected and may represent the primary damage mechanism for anatase coatings.

In addition to dynamic studies of the laser damage process by means of time resolved Raman spectroscopy (TRRS), spatially resolved Raman measurements of localized equilibrium damage (25 μm resolution) will also be reported.

2.0 EXPERIMENTAL SECTION

2.1 OPTICAL COATINGS

All TiO_2 and ZrO_2 dielectric coatings were prepared by reactively sputtering titanium or zirconium in Ar+/O atmospheres in an rf diode system onto 25 mm dia fused silica substrates. The crystalline phase of a deposited

coating was controlled by appropriate choice of sputtering parameters; details appear in the literature (Refs. 9 and 10). Microcrystalline grain sizes were ca 50 mm and coating thicknesses varied from 0.1 μm to over 5 μm.

2.2 RAMAN MEASUREMENTS

Raman spectra were excited at normal incidence using the 180 deg back-scattering geometry depicted in Fig. 6. The sample was held in a micro-positioning stage having spatial resolution of several micrometers. Scattered light was collected at f/1.4 and imaged onto the slits of a SPEX 0.85 m double monochromator. Dispersed radiation was detected by an RCA C31034-01 PMT and signals were processed by conventional photon counting electronics.

A gated intensified diode array detector was used to record spectra in a time resolved mode. In this instance, only the entrance slits of the monochromator were used; to reject Rayleigh scattered light under these conditions a special notch filter tuned to reject the probe laser wavelength was inserted in front of the entrance slits. Each notch filter (Omega Optical) had a rejection band of 15 nm centered around the primary Raman probe wavelengths of 488 and 532 nm.

Three different laser beam excitation arrangements were used. Equilibrium laser damage measurements at room temperature required colinear Ar+ Raman probe and Nd:YAG damage beams focused onto the sample surface. The 488 nm CQ Ar+ probe beam operating at 200 mW had a 50 μm spot size while the 532 nm pulsed Nd:YAG damage beam operating from 1-50 mJ/pulse had a 500 μm spot size. (Measured pulse widths were 10 ns.) The second arrangement required combining the 10.6 μm CW CO_2 beam used to heat samples appreciably above room temperature with the 532 nm Nd:YAG pulsed beam operated at a low pulse energy as the Raman probe. Sample temperatures were measured by means of a two color optical pyrometer. The final arrangement used the Nd:YAG laser to both create damage and act as the Raman probe as shown in Fig. 7.

A pellicle beamsplitter served to split individual pulses into a primary and secondary pulse which contained ca 10 percent of the primary pulse energy. Figure 7 also shows the electronic delay schematic designed to open the array detector at selectable times following arrival of the damage pulse at the sample. The detector bandwidth was maintained at 8 ns for all measurements and was controlled by means of the Avtech Model AVL-V-TN1 pulse

generator which was triggered by an electronic signal from the pulsed Nd:YAG laser (Quantel Model #580) that preceded the output laser pulse by an adjustable time. Spectra were read from the detector by a TN-1710 multichannel analyzer and stored on floppy disk for future reference. All measured spectra were normalized to the broadband optical response of the notch filter, monochromator and detector.

3.0 RESULTS

Optical coatings which have incurred irreversible laser damage exhibit features similar to those seen in micrographs of single and multilayer anatase coatings that have been subjected to intense pulsed 532 nm radiation (Fig. 8). Evidence for coating ablation and recrystallization is apparent in each picture; however, more homogeneous damage centers are produced following multiple laser shot exposure over the same area. Damage is fairly uniform over the irradiated areas which have average diameters which range from 250 to 750 μm. With proper optics, a Raman probe laser beam can be focused to a 1 μm spot size enabling surface profiling of the damaged region with regard to identification of crystalline phases, decomposition products, and coating thickness measurements. Results of such spatially resolved measurements in addition to in situ Raman measurements obtained in a time resolved mode are discussed below.

3.1 EQUILIBRIUM DAMAGE-SPATIALLY RESOLVED STUDIES

3.1.1 ROOM TEMPERATURE MEASUREMENTS

Thin film TiO_2 optical coatings have been characterized with regard to phase identity and homogeneity by Raman spectroscopy. The Raman spectrum of a thin anatase film on silica is depicted in Fig. 4. By analyzing the $Z(X\ Y)\bar{Z}$ component of the scattered radiation, Raman scattering from the silica substrate is markedly attenuated at frequencies below 800 cm^{-1}. The broad feature at ca 800 cm^{-1} is, however, assigned to Raman scattering from the glass substrate. For the other scattering geometry $Z(X\ X)\bar{Z}$ substrate features overwhelm Raman lines from the thin optical coatings. Therefore, in all subsequent measurements, the $Z(X\ Y)\bar{Z}$ scattering geometry was used. The major anatase lines at 145, 199, 398, 517 and 639 cm^{-1} and rutile features at 244, 440 and 610 cm^{-1} previously assigned clearly distinguish the two crystalline phases (Refs. 11 and 12).

The equilibrium damage state was characterized by Raman measurements of both anatase and rutile optical coatings subjected to 532 nm pulsed irradiation from an Nd:YAG laser. When the damage threshold for rutile coatings was exceeded, measured Raman spectra at long times following the damage pulse were qualitatively similar to the undamaged coatings; however, band intensities were lower than for the undamaged samples (Fig. 9). While no change in crystalline phase was detected, the lower band intensities indicate removal of TiO_2 by the damage laser pulse. Since Raman band intensities correlate with coating thickness, depth profiling of the damaged area is possible and has been determined for several samples.

Subtle changes in band positions and bandwidths were observed in Raman spectra of anatase coatings following the damage pulse. As seen in Fig. 10, all major features are significantly broadened and reduced in intensity. The major 145 cm^{-1} band appears at the higher frequency following damage while features above 300 cm^{-1} appear at slightly lower frequencies. Following damage, the 398 cm^{-1} band shows a weak shoulder at higher frequencies, and the 639 cm^{-1} band appears broadened to the low frequency side. These are regions where Raman scattering attributed to the rutile phase is expected.

The 145 cm^{-1} band has been observed to increase in frequency as a function of increased hydrostatic pressure (Ref. 13). An increase in frequency for this mode is also observed following damage by a single 532 nm pulse near threshold damage energy. Based on pressure dependent measurements, the observed frequency shift can be correlated with an imposed pressure of 10 kbar. Therefore, results can be interpreted in terms of a laser induced pressure wave which distorts the crystalline lattice, thereby, locking in the high pressure (higher density) phase. Continued laser damage at this damage zone is eventually expected to form a stable high density phase of TiO_2. Figure 11 shows substantial rutile content in the damage zone following multiple laser pulse damage to the same area.

Results from such measurements suggest that for a constant laser damage energy and similar coating thickness, rutile coatings appear to have a significantly higher damage threshold than anatase coatings. In addition, the extent of coating removed depends on the laser pulse energy and coating thickness. Multiple pulses on the same area remove successively less and less coating eventually converging to a limit. The 488 nm Ar+ probe laser

(1 W CW) was found not to damage these rutile or anatase coatings even when focused to a 50 μm spot size at the sample.

Mixed rutile/anatase coatings also appear to damage more readily than pure rutile coatings alone. Following damage, the rutile/anatase ratio has significantly increased suggesting selective transformation of anatase to rutile.

Finally, the applicability of using Raman spectroscopy to spatially profile the laser induced damage zone is demonstrated in Fig. 12. The intensity ratio of the 145 cm^{-1} band before and after damage is plotted as a function of distance from the damage zone center. For this measurement, the probe laser spot size was 25 μm in diameter and the damage zone had a diameter of 500 μm. Higher resolution is possible (1 μm) with proper focusing optics. The intensity ratio corresponds to a relative coating thickness measurement; however, the technique could also be used to profile the phase composition across the damage zone in cases where multiple crystalline or amorphous phases are known to exist.

3.1.2 HIGH TEMPERATURE MEASUREMENTS

The effect of temperature on phase stability of sputtered TiO_2 optical coatings was investigated using 10.6 μm radiation from a CW CO_2 laser as a heating source. For this measurement, a colinear pulsed Nd:YAG laser operated at low pulse energy served as a Raman probe. To suppress sample blackbody emission at high temperatures, a gated detection scheme was used and the detector opening was synchronized to the laser pulse. Since the normal Raman effect is a spontaneous process, effective rejection of sample blackbody radiation at high temperature is achieved.

Rutile coatings exhibited no phase changes during heating to nearly 1500°C. However, significant band shifts to lower frequency were measured. For instance, the a_{1g} mode at 610 cm^{-1} at initial room temperature spectrum is recovered as shown in Fig. 13.

Anatase coatings exhibited a rather different response to temperature as shown in Fig. 14. An irreversible phase transition to the rutile crystalline form occurs at a temperature below 910°C. This is consistent with equilibrium thermodynamics which predicts a phase transition in this temperature region. However, when the coating is cooled down to room temperature,

the rutile phase persists. The phase change is accompanied by a significant change in density, which leads to swelling and eventual microcrack formation in the coating.

Other oxidic coating materials also undergo reversible phase transformations as a function of temperature as shown in Fig. 15 for a ZrO_2 coating on a metal substrate. The monoclinic, tetragonal and cubic phases of this material exhibit unique Raman spectra that characterize each phase.

3.2 TRANSIENT MEASUREMENTS-TIME RESOLVED RAMAN SPECTROSCOPY

The Raman experiments discussed previously were designed to characterize equilibrium damage to optical coatings induced by pulsed high energy laser irradiation. A second group of experiments was performed to characterize the nonequilibrium state immediately following irradiation by a high energy laser pulse in a regime where equilibrium thermodynamics does not apply. The first series of experiments involved measuring Raman spectra separated in time by increments of 10 ms following the 532 nm Nd:YAG laser damage pulse. The 488 nm CW Ar+ laser line was used as the Raman probe. Below damage threshold for any coating Raman spectra acquired at 10 ms intervals are identical. When anatase coatings incur damage, a rapid intensity rise near the exciting line is observed; however, the major anatase lines are still evident albeit at lower intensity in all subsequent spectra. Results for rutile coatings are shown in Fig. 16. At 10 ms following the damage pulse, the low frequency intensity rise is evident. However, the rutile vibrational lines are not seen. Rather, the 640 cm^{-1} e_g anatase line is observed. At longer times, the rutile spectrum recovers, again at a lower intensity than the undamaged coating. An apparent reversible phase transition to an anatase-like phase has occurred.

This experiment was repeated using 1064 nm pulsed radiation from a Nd:YAG laser to create surface damage, and the 488 nm Ar+ laser line to probe the damage site. (The damage and probe beam were combined at a multi-element air-spaced etalon.) Spectra recorded at 10 ms intervals exhibited the same trends as observed using the frequency doubled 532 nm line from the Nd:YAG laser to create laser damage in the coating.

The existence of an anatase-like phase at short times following laser damage to rutile coatings is further supported by data depicted in

Fig. 17. Spectra were recorded as a function of a detector delay for a single Nd:YAG laser pulse that served to both induce damage and act as the Raman probe. Spectra were acquired for detector delays up to several hundred nanoseconds. Evidence of an anatase-like phase persists even at detector delay times in excess of several hundred nanoseconds. At lower pulse energy below damage threshold conditions, only the rutile spectrum is measured at zero detector delay. For longer detector delay times, no Raman signal can be detected.

Similar results have been observed using optically delayed laser pulses of high (damage) and low (probe) energy separated in time. With no delay between damage and probe beams, the 640 cm^{-1} band is observed in both Stokes and anti-Stokes spectra verifying that it is indeed a vibrational feature. The reversible transformation from the starting rutile phase to an anatase-like phase must occur rapidly. Stokes and anti-Stokes spectra recorded using a probe pulse delayed in time by 20 nm still reveal the 640 cm^{-1} band. However, at long times following the damage event, the rutile spectrum has completely recovered, and no trace of the 640 cm^{-1} anatase line is observed.

4.0 MECHANISTICS OF LASER DAMAGE TO TiO_2 COATINGS

Measured Raman spectra under equilibrium and nonequilibrium conditions provide sufficient structural information to formulate a model for the laser damage process in TiO_2 optical coatings. The relative instability of anatase coatings under laser damage conditions results from the observed irreversible phase transformation to the rutile phase at temperatures below 910°C. Localized heating from the laser damage pulse stimulates the phase transition. Induced swelling at the damage spot leads to lattice mismatch and localized fracturing of the surface. Vestiges of the rutile phase are transported away from the damage center. The remaining anatase, not having enough thermal energy to change phases, persists at long times exhibiting lower intensity Raman lines than the undamaged starting material.

A slightly different mechanism is proposed to explain laser damage phenomena in rutile coatings, which exhibit a higher damage threshold than the anatase coatings. The rutile phase undergoes no detectable phase transition at temperatures below ca 1500°C. Raman observed band shifts to lower

frequencies indicate localized bond length increases which can result in bulk swelling. These changes are reversible, however, and should not contribute to the damage process. However, time resolved Raman measurements reveal features characteristic of the anatase phase for spectra acquired soon after the damage laser pulse has encountered the surface. Since this phase transition (rutile-anatase) does not occur under equilibrium conditions, a nonequilibrium explanation is in order.

High energy laser irradiation of materials can give rise to electronic excitation through multiphoton processes (Ref. 14). Vibrational energy levels may still be populated as in the ground state since the excitation process is rapid. Time resolved measurements will then probe the excited electronic state.

An elementary molecular orbital treatment of titanium localized in an octahedral oxygen environment suggests that the filled sigma bonding molecular orbitals between titanium and oxygen ligands are of a_{1g}, t_{1u} and e_g symmetry (Ref. 15). Theoretical band structure calculations for rutile conclude that the upper valence band has a predominant O-2p orbital character whereas the conduction band of TiO_2 is derived mainly from Ti-3d states (Ref. 16). Therefore, excitation of a bonding electron from the highest occupied e_g state to an antibonding t_{1u}* state which is strongly allowed would tend to weaken the bonding between titanium and oxygen. Electron repulsion effects would act to perturb the octahedral structure forcing the square planar oxygen arrangement to distort. The resulting puckered structure in the excited state of rutile is qualitatively similar to the structure of the anatase ground state. Therefore, the Raman spectrum of the excited rutile state should exhibit similar features to the normal Raman spectrum of anatase. When the excited electron relaxes back to the ground state, the rutile structure is recovered. In this nonequilibrium case, the electronic transition causes a phase change as opposed to the equilibrium thermally induced phase change for anatase. The higher damage threshold of rutile coatings may result from the fact that a significant amount of the laser damage energy is stored in the excited electronic state, whereas in anatase, the energy may rapidly be thermalized leading to the irreversible phase transformation.

The persistence of the Raman spectrum of laser damaged rutile coatings at times approaching several hundred nanoseconds following the damage pulse may be explained in terms of resonance enhancement of the vibrational band intensities. It has been demonstrated that under resonance excitation of I_2, Raman spectra can be recorded from a single laser pulse at detector delay times approaching 1 ms (Ref. 17). A similar mechanism is reasonable when electron excitation is induced in solids by laser irradiation. Figure 18 shows the intensity variation of the 530 cm^{-1} anatase-like band in a rutile coating during laser induced damage as a function of detector delay time. These results are in qualitative agreement with predictions given in Ref. 17.

An alternate explanation involves surface wave trapping of the laser damage pulse. If no damage is created by an incident laser pulse, spontaneous Raman scattering will occur with no measurable Raman signal detectable following the laser pulse. If, however, the dielectric coating is damaged, the laser pulse can become trapped between coating and substrate undergoing multiple internal reflection and producing Raman scattering during the time the pulse is trapped. To test this idea, additional measurements will have to be made on laser damaged coatings.

5.0 CONCLUSIONS

Raman studies of laser induced damage in TiO_2 optical coatings were undertaken to provide molecular structural information for understanding the damage process. Anatase coatings, determined to have a lower damage threshold than rutile, fail by virtue of an irreversible phase transition to the rutile structure at temperatures below 910°C. Rutile accommodates energy in an excited electronic state resulting in a nonequilibrium phase transformation to an anatase-like state. Both coatings apparently fail by selective removal of the anatase phase from the coating.

In addition to structural considerations of the coating, substrate effects may also be important in understanding the mechanism responsible for coating failure. Figure 19 shows measurable damage to a silica substrate as a function of the number of laser shots. The laser induced polarization intensity changes result from microscopic surface damage (microcracks, density fluctuations) which act to scramble the polarization of the probe laser beam.

Substrate damage could lead to optical coating failure by other mechanisms and suggests another topic for additional work in this area. Raman techniques will be applied to laser damage studies of other coatings such as ZrO_2 and multilayer designs in future work where attention to the coating-substrate interaction will also be focused.

Preliminary measurements for single layer ZrO_2 coatings on metal substrates are shown in Fig. 20. Raman spectra are recorded as a function of relative laser pulse energy at 532 nm. As the pulse energy increases, reversible transformation from monoclinic ZrO_2 to tetragonal ZrO_2 to cubic ZrO_2 (a single Raman line near 550 cm^{-1}) can be discerned. The existence of multiple phases suggests similar failure mechanisms as observed for TiO_2 coatings but further work is necessary to confirm these ideas.

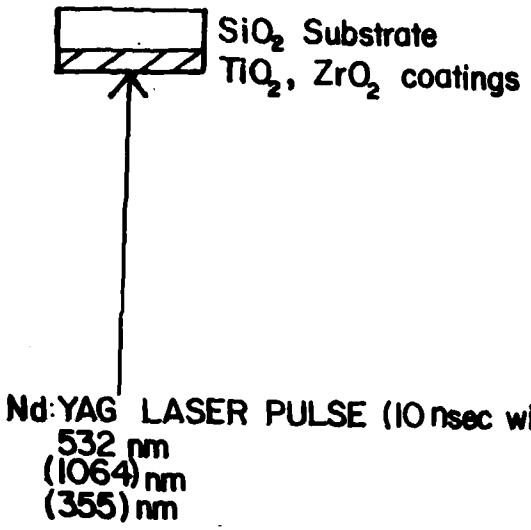

DAMAGE MECHANISM

1. Rapid Energy Deposition ($< 10^{-12}$ sec)
   a. Impurity Absorption
   b. Multiphoton Excitation
2. Energy Partitioning to Vibrational Modes (10^{-12} sec $< t < 10^{-8}$ sec)
   a. Surface Heating
   b. Localized Melting
   c. Material Ablation
3. Recovery–De excitation (10^{-8} sec $< t < 10^{-2}$ sec)
   a. Decomposition
   b. Surface Cooling
   c. Recrystallization
   d. Phase Changes
   e. Macroscopic Surface Relaxation

Figure 1. Hypothetical laser damage mechanisms with estimated relaxation times.

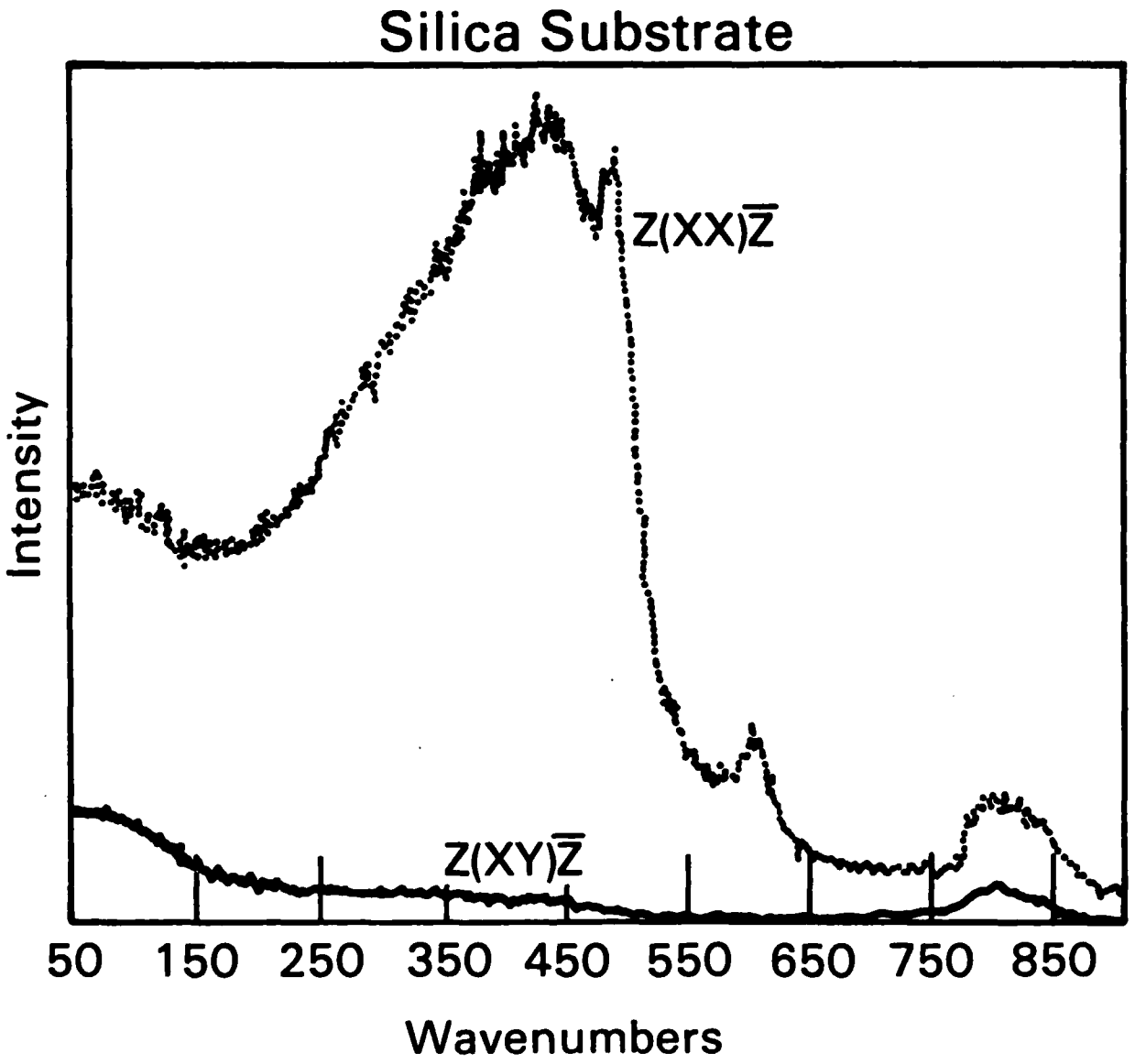

Figure 2. Raman spectra of an uncoated vitreous SiO_2 substrate. The standard scattering geometry designation is based upon a coordinate system defined at the sample where Z and $\bar{Z}$ are the incident and scattered laser directions and X and Y define which component of the electric field is transmitted by the analyzer.

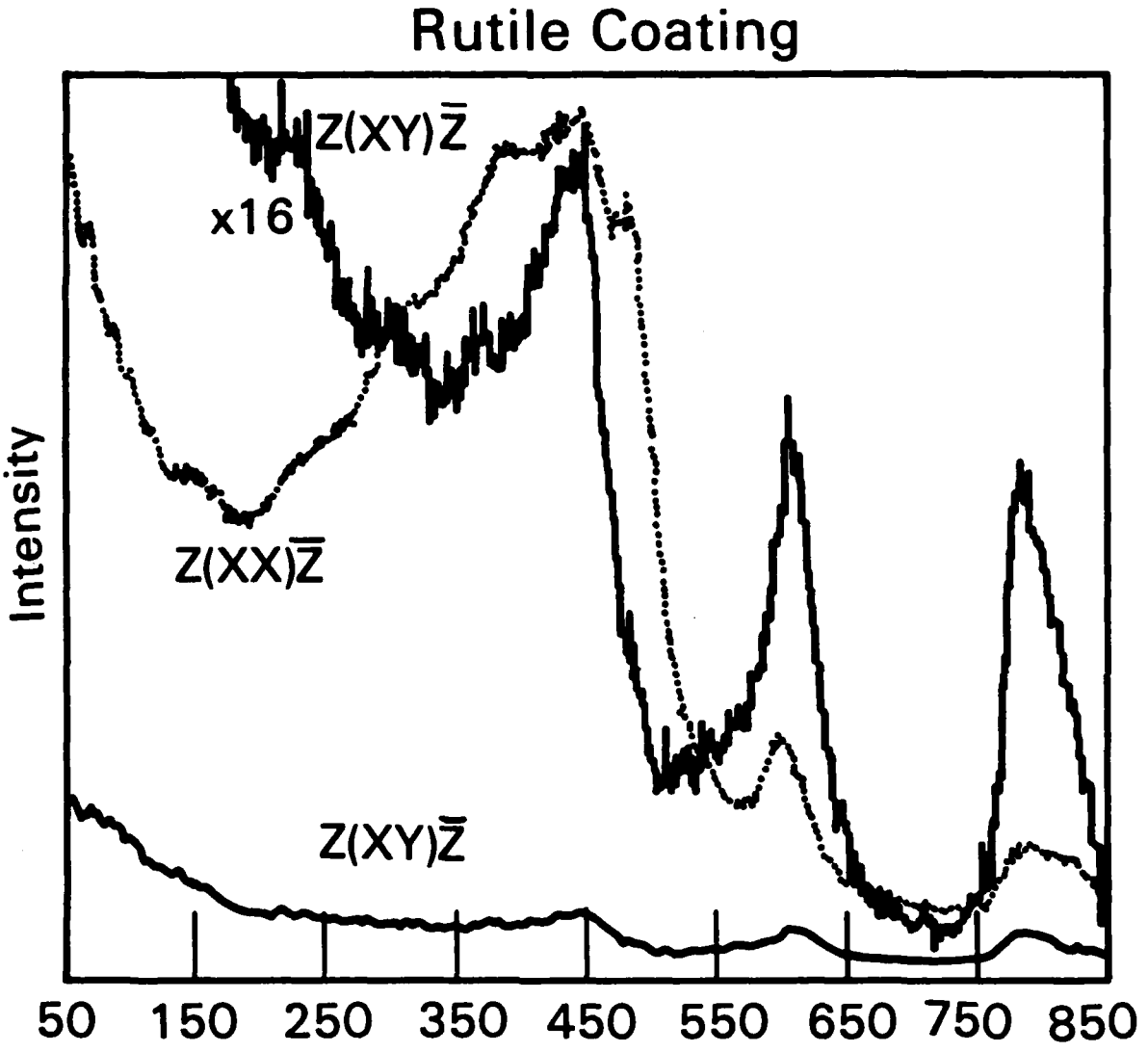

Figure 3. Raman spectra of a 1592°A thick rutile (TiO_2) coating on SiO_2.

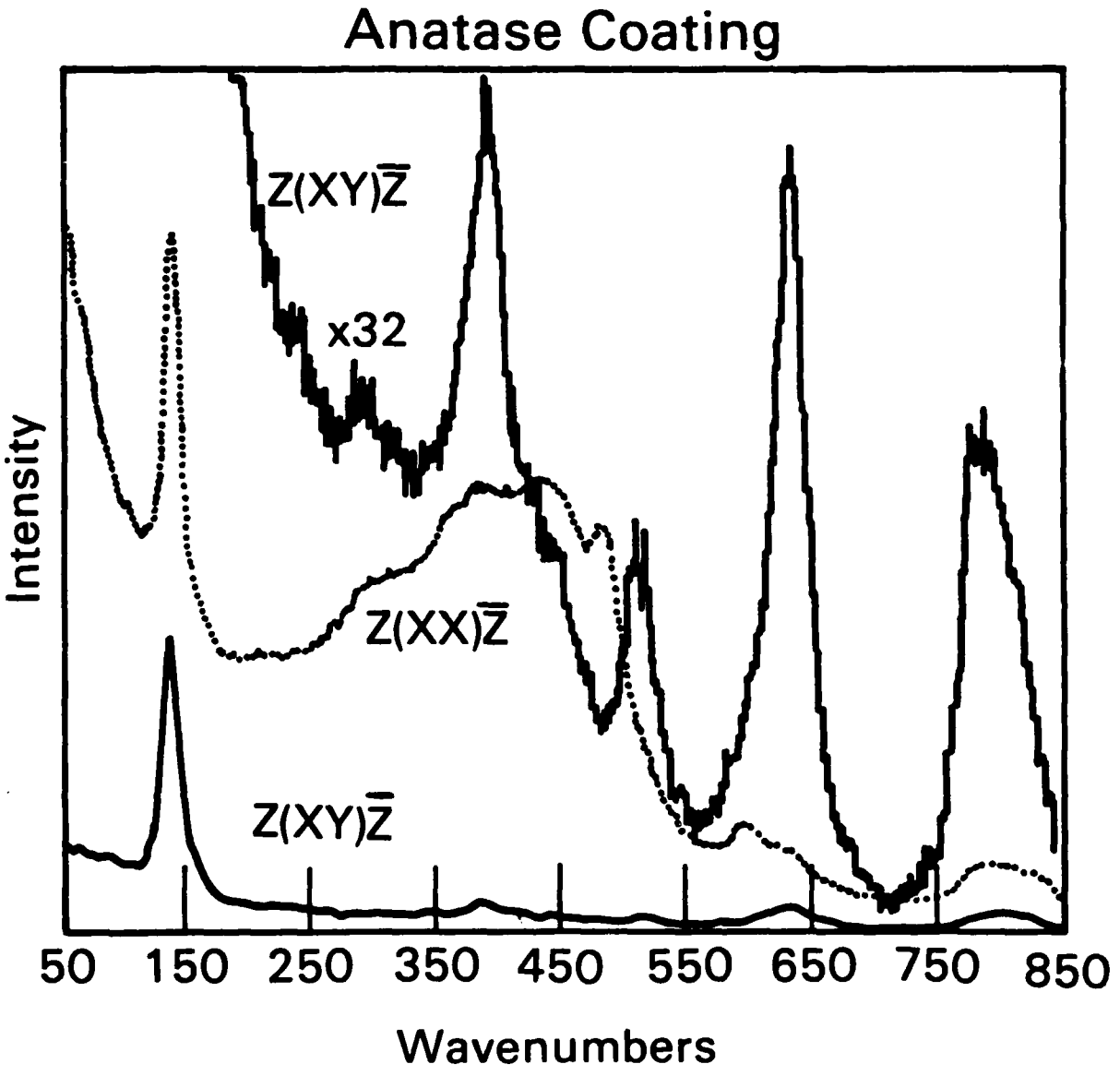

Figure 4. Raman spectra of a 1811° A thick anatase (TiO_2) coating on SiO_2.

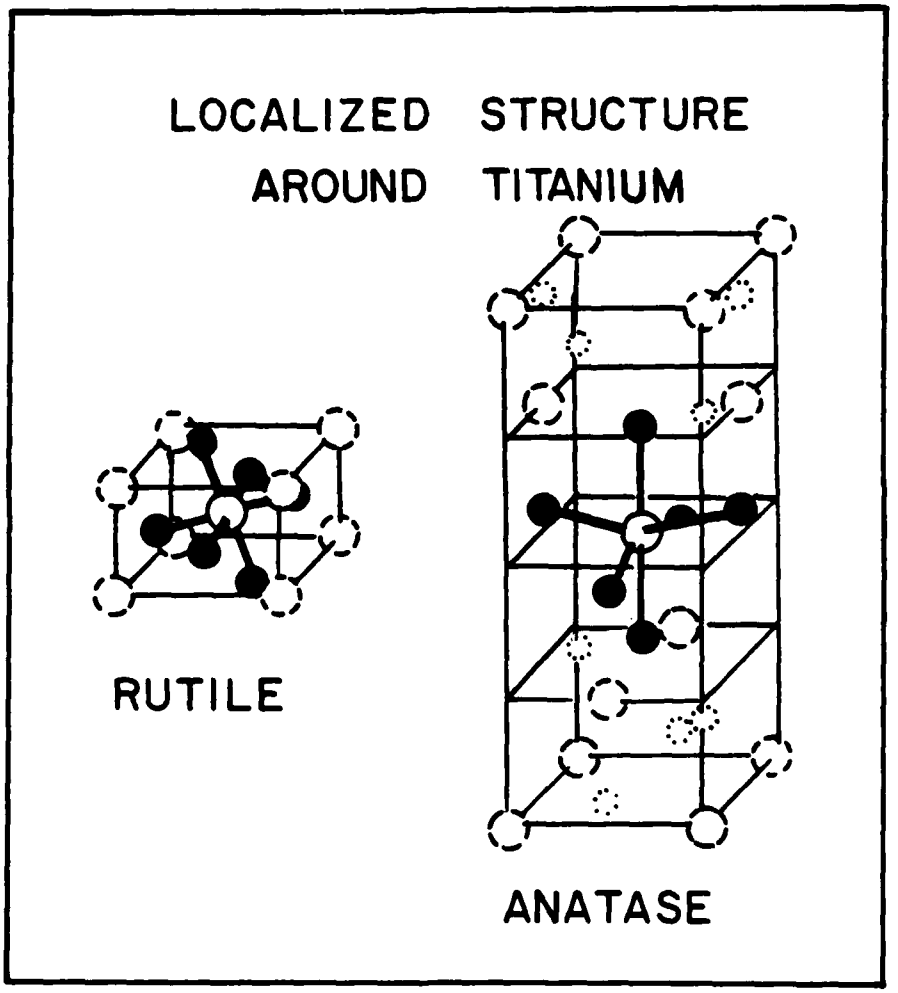

Figure 5. Localized molecular structures of rutile and anatase phases of TiO_2.

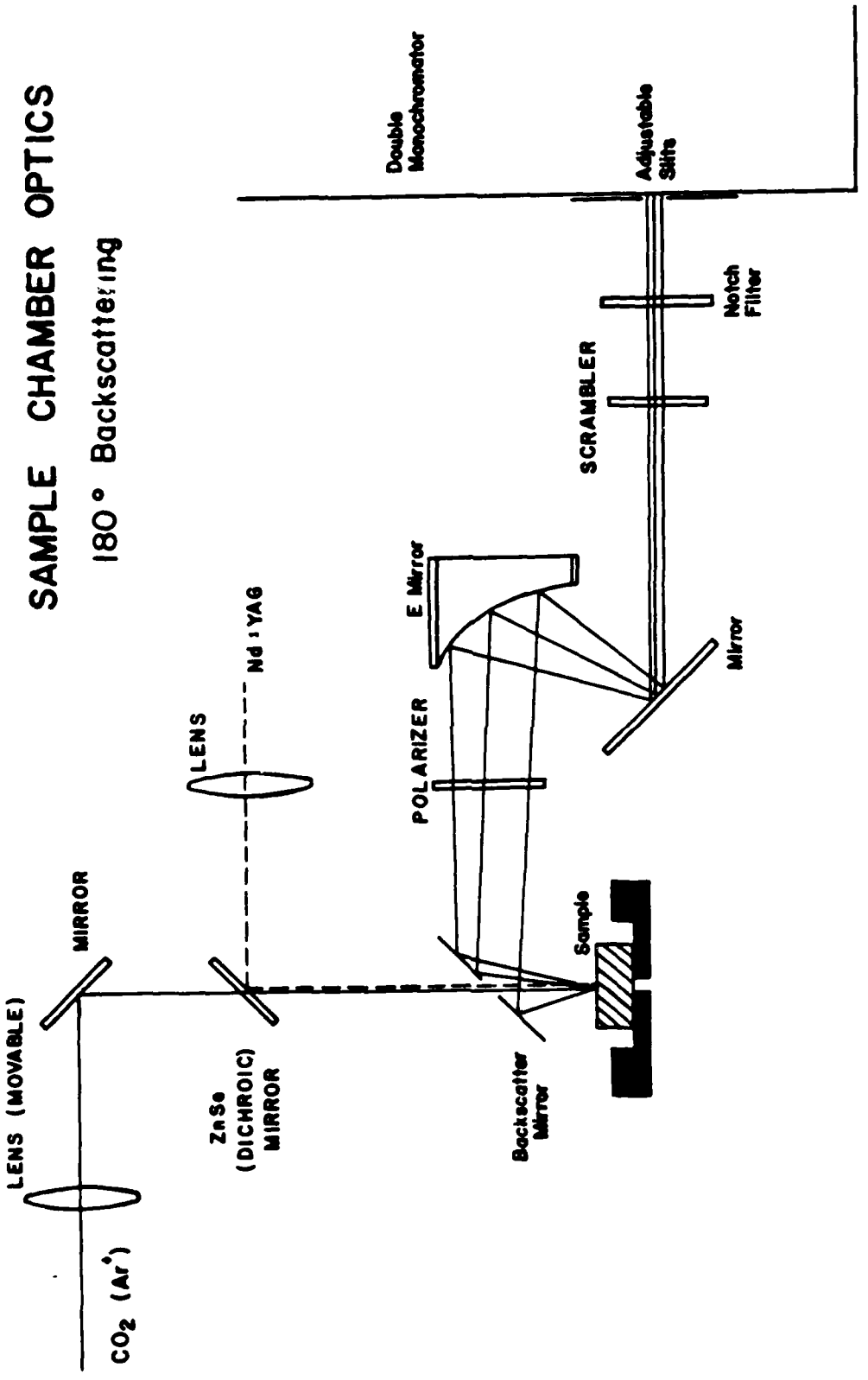

Figure 6. Backscattering geometry for raman experiment with damage/heating and probe beams colinear.

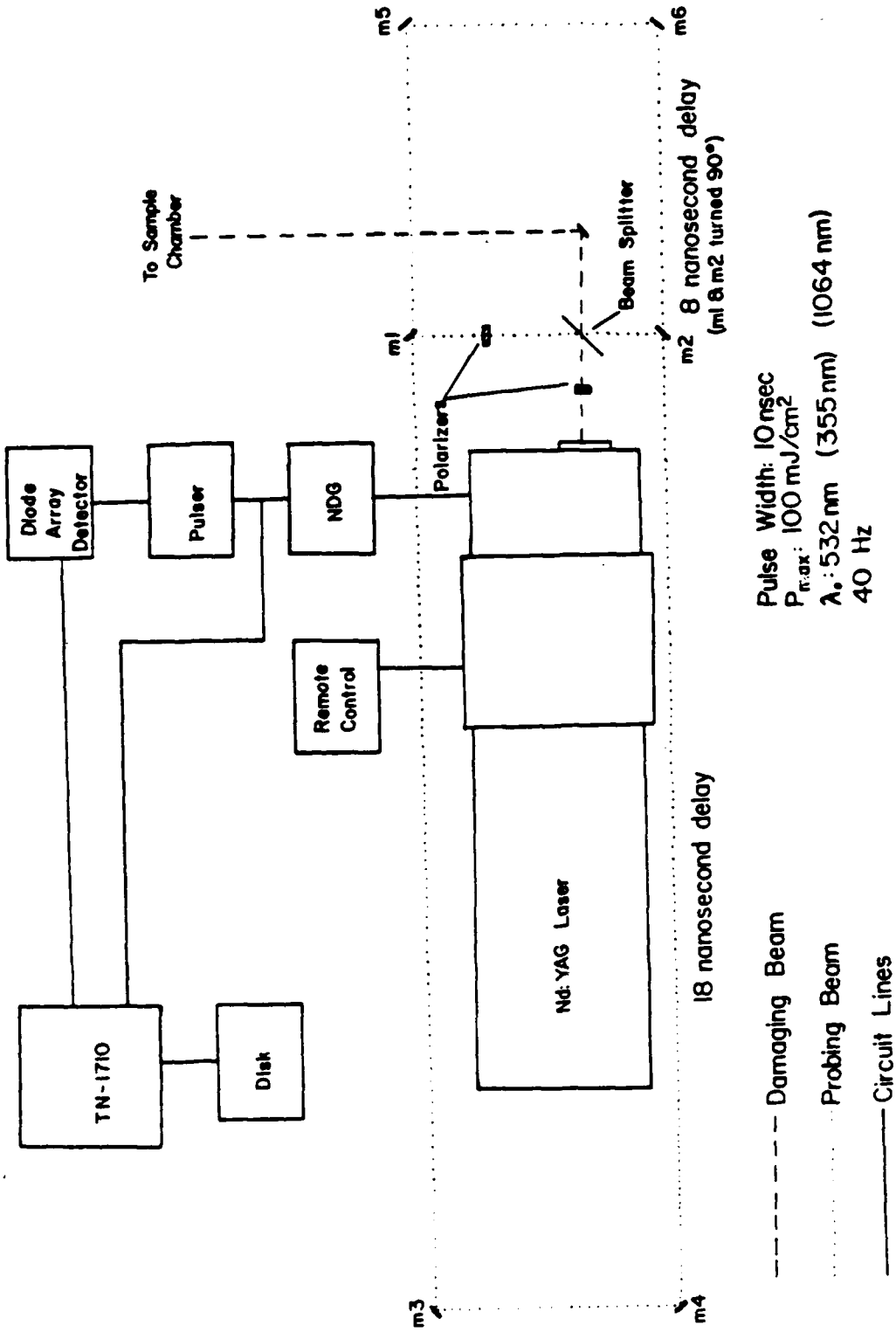

Figure 7. Signal delay schematic showing optical delay path. (NDG refers to a nanosecond delay generator.)

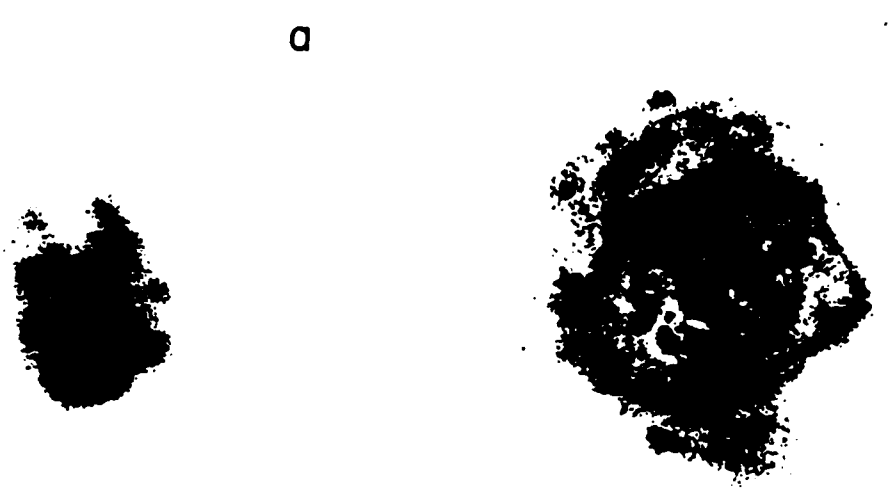

Single layer anatase coating (0.8 μm). 1 shot.

Multilayer anatase coating. 1 shot.

Single layer anatase coating. Multiple shot damage.

Multilayer anatase coating. Multiple shot damage.

Figure 8. Photomicrographs of TiO_2 coatings subjected to pulsed 532 nm irradiation above damage threshold (100X magnification).

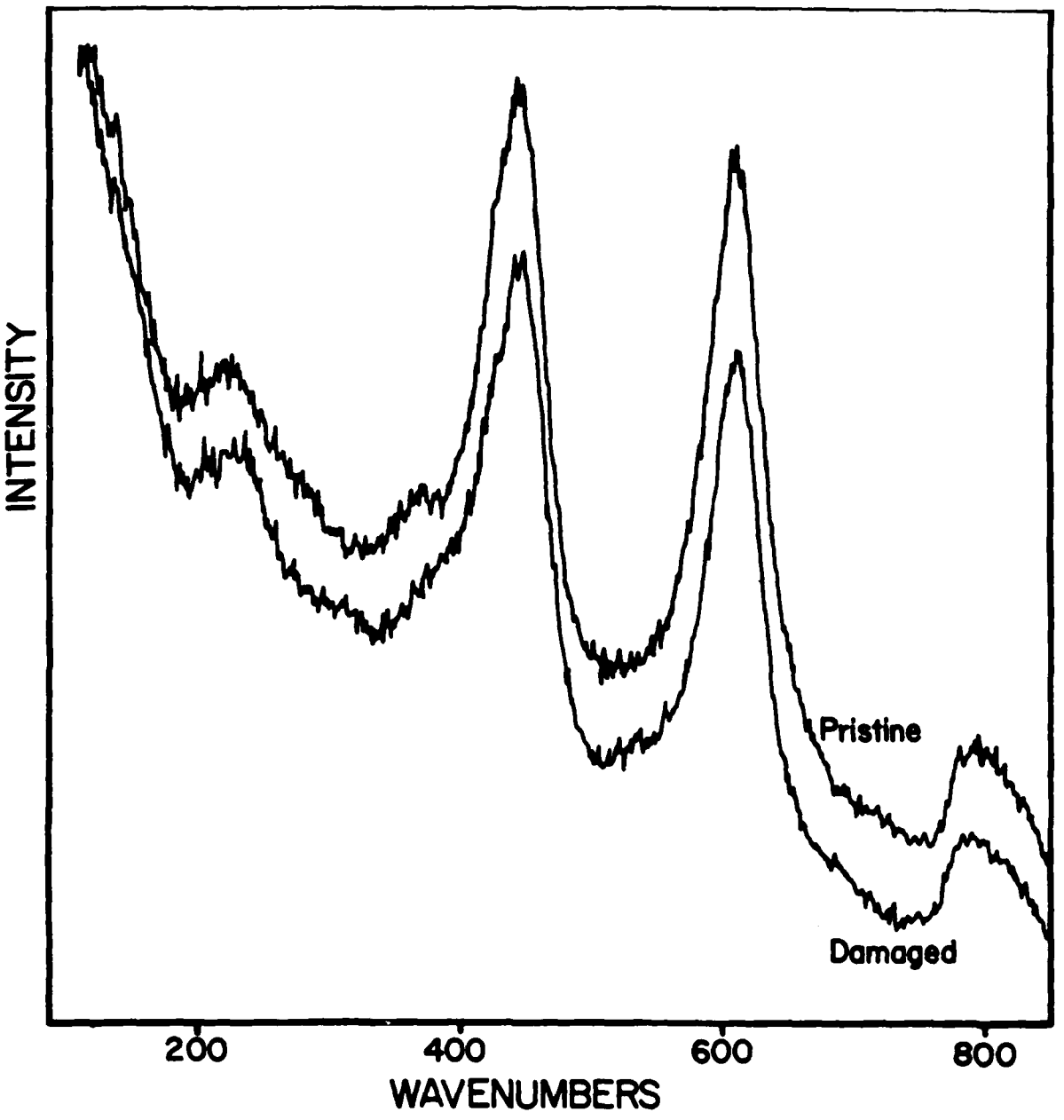

Figure 9. Laser induced damage in a single layer (0.9 μm) TiO_2 (rutile) coating on silica.

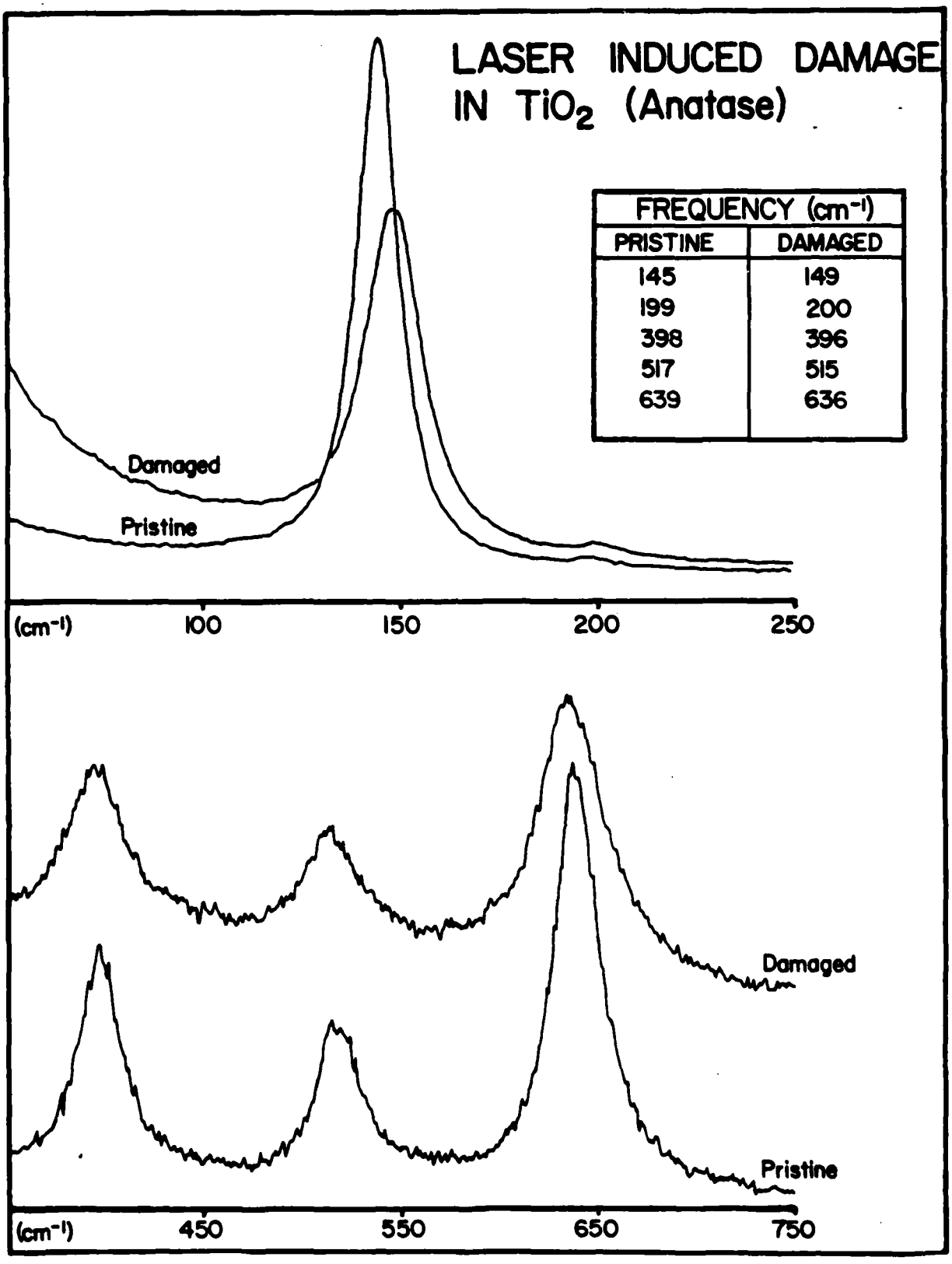

Figure 10. Raman spectra of a 9587°A anatase film on silica before and after exposure to a single 532 nm high energy pulse.

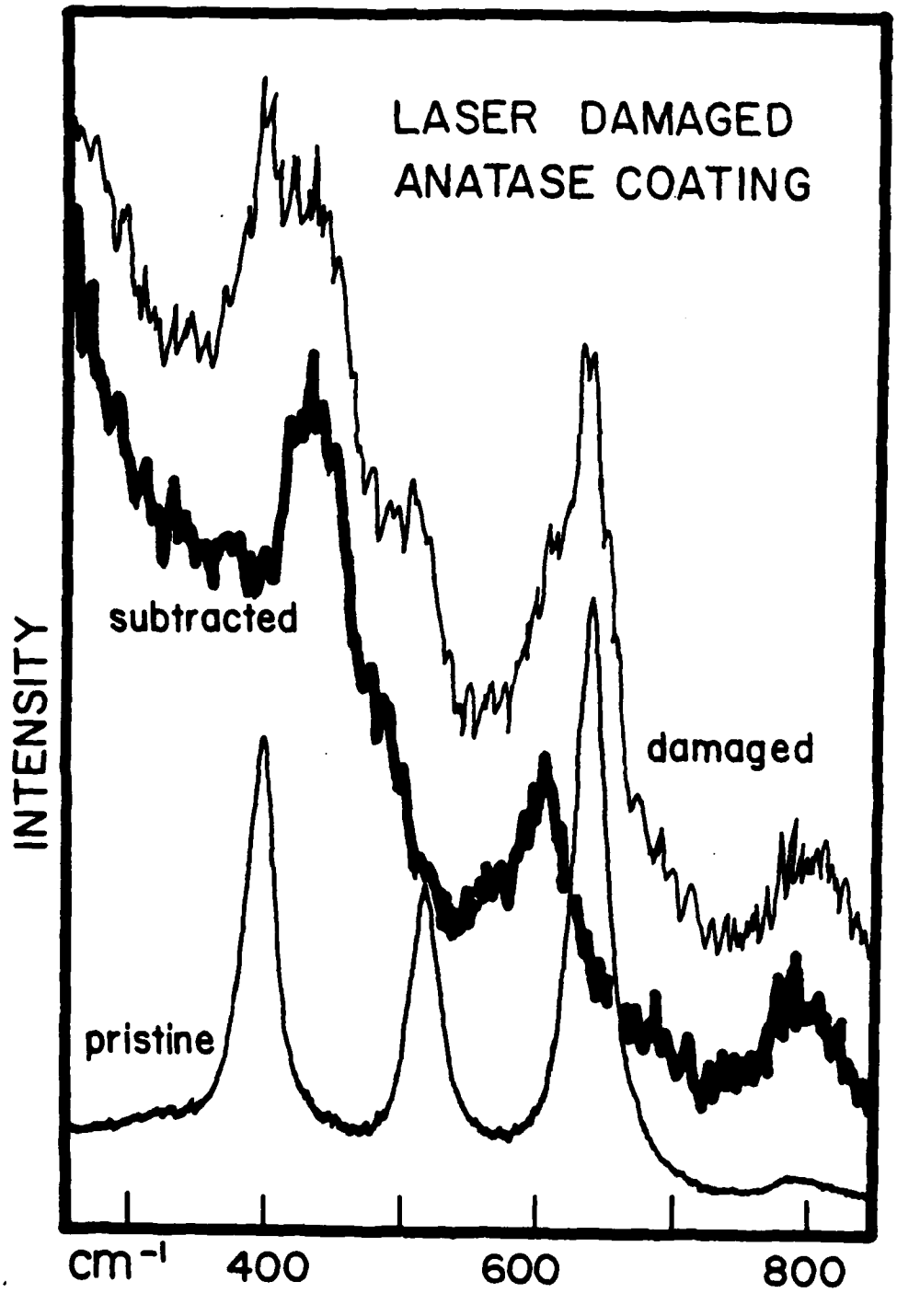

Figure 11. Raman characterization of multiple laser pulse damage to a 9587°A single layer anatase coating.

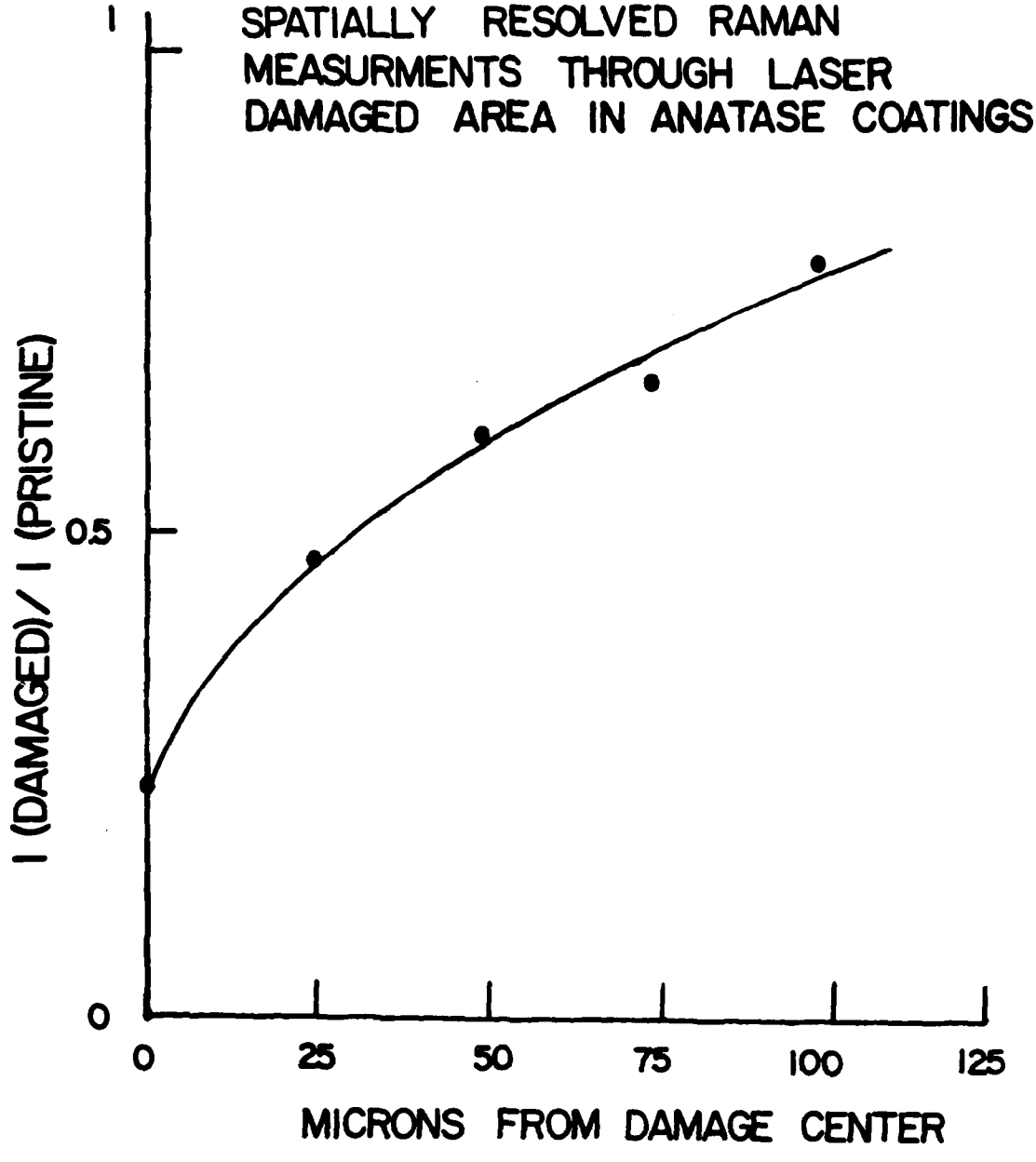

Figure 12. Raman characterization of multiple laser pulse damage to a 9587°A single layer anatase coating.

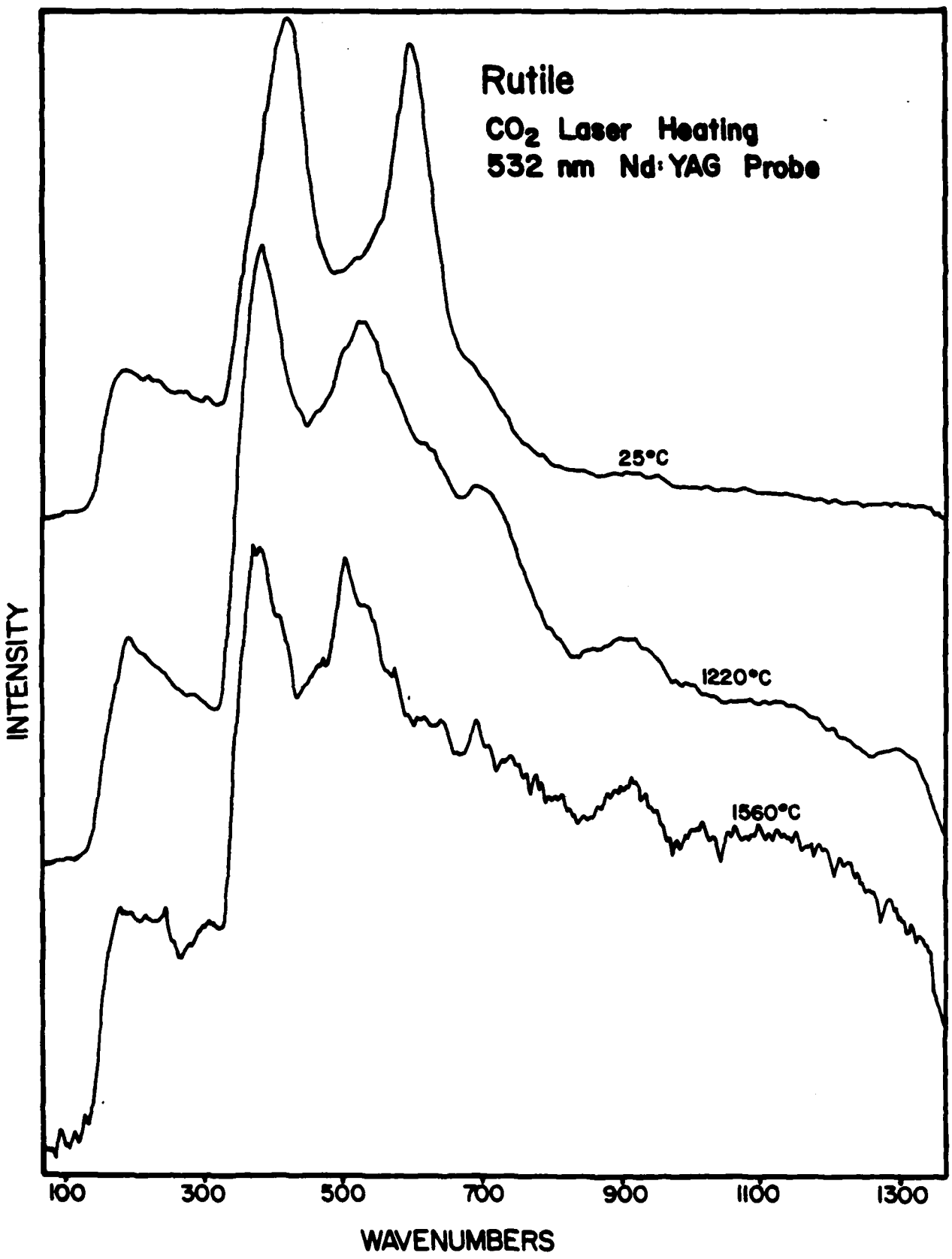

Figure 13. Temperature dependent raman spectra of rutile using a CO_2 laser as the localized heating source.

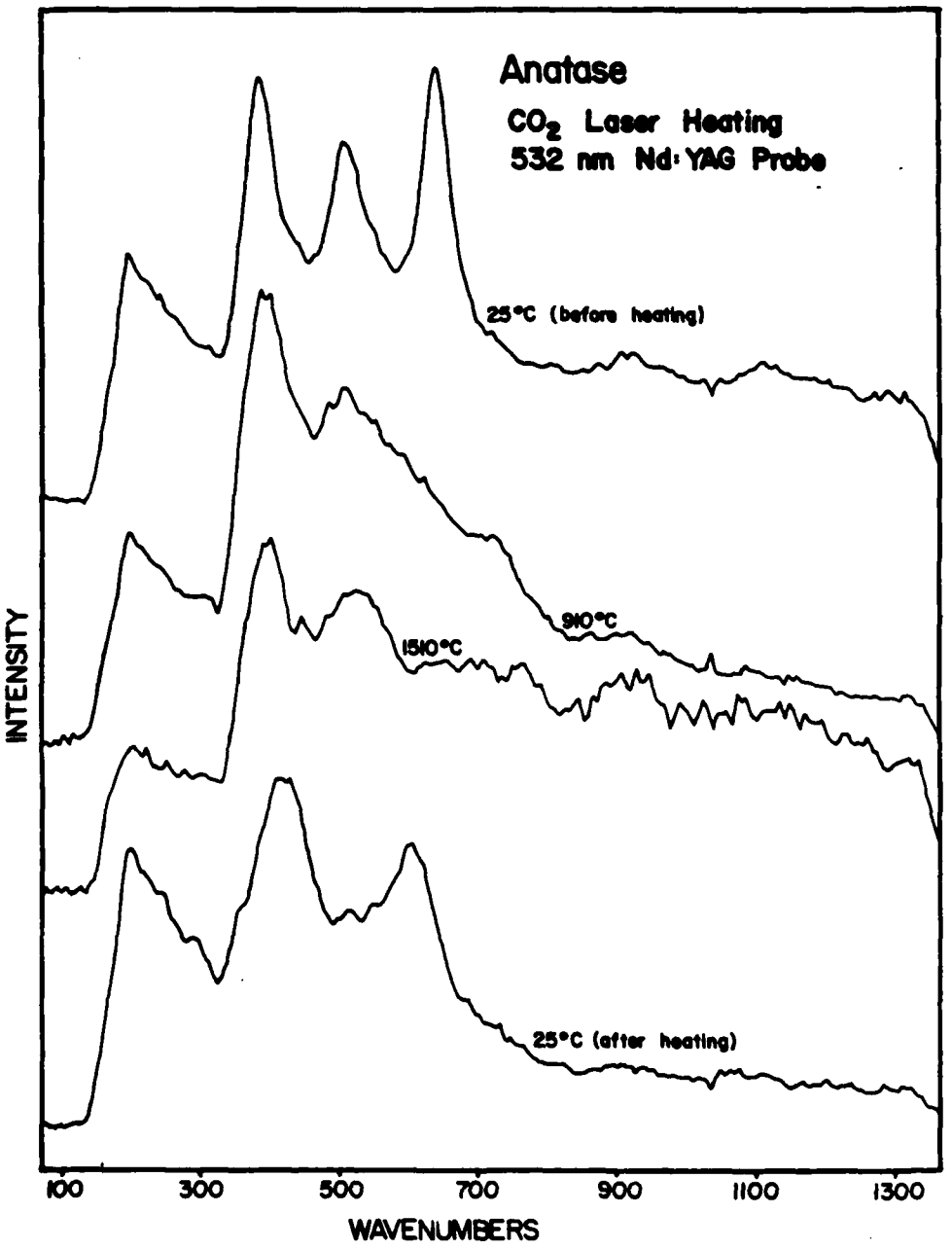

Figure 14. Raman spectra taken during an equilibrium CO_2 laser heating experiment showing irreversible transformation of anatase to rutile at ca, 901°C.

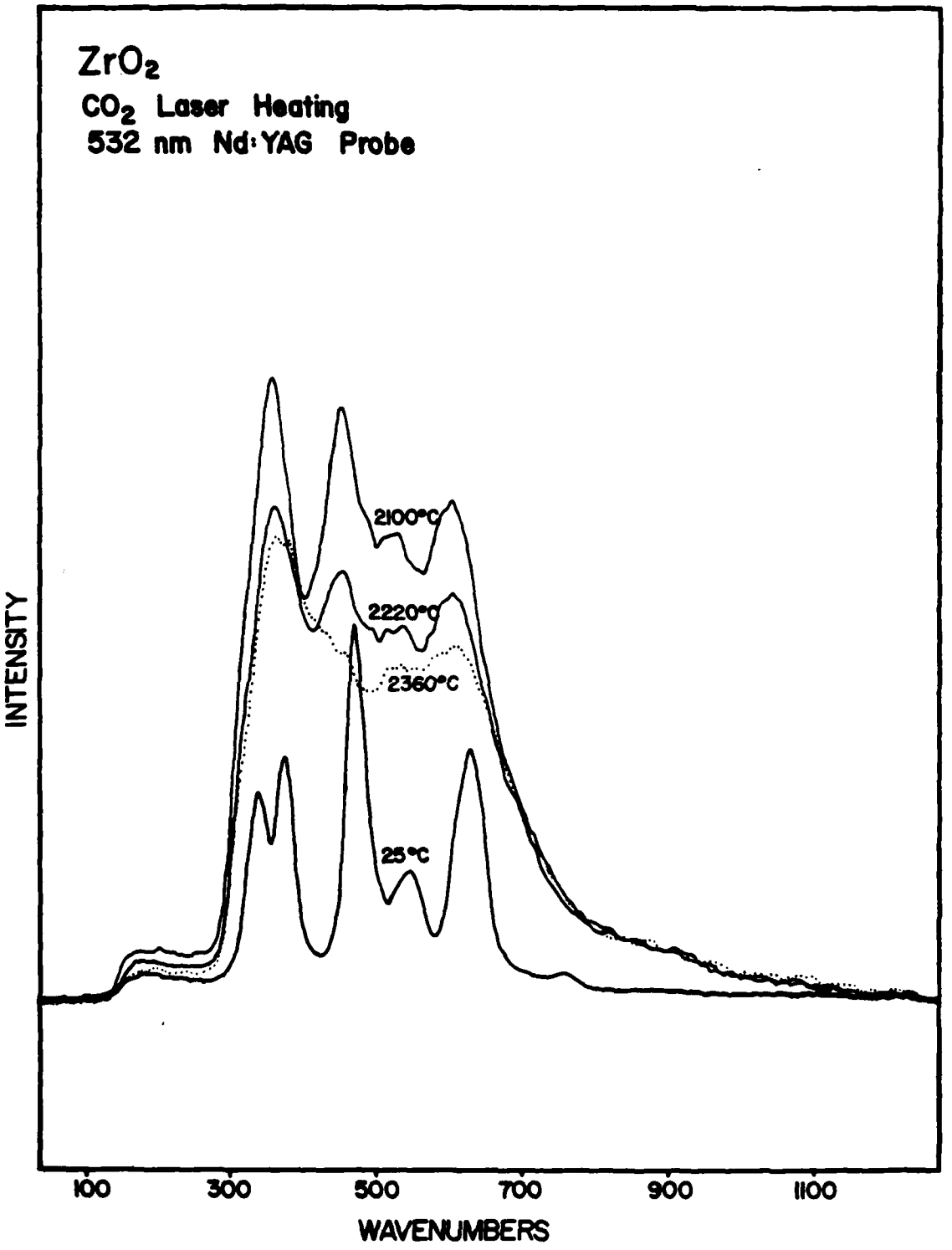

Figure 15. Reversible phase transformations in CO_2 laser heated ZrO_2 deposited on a metal substrate.

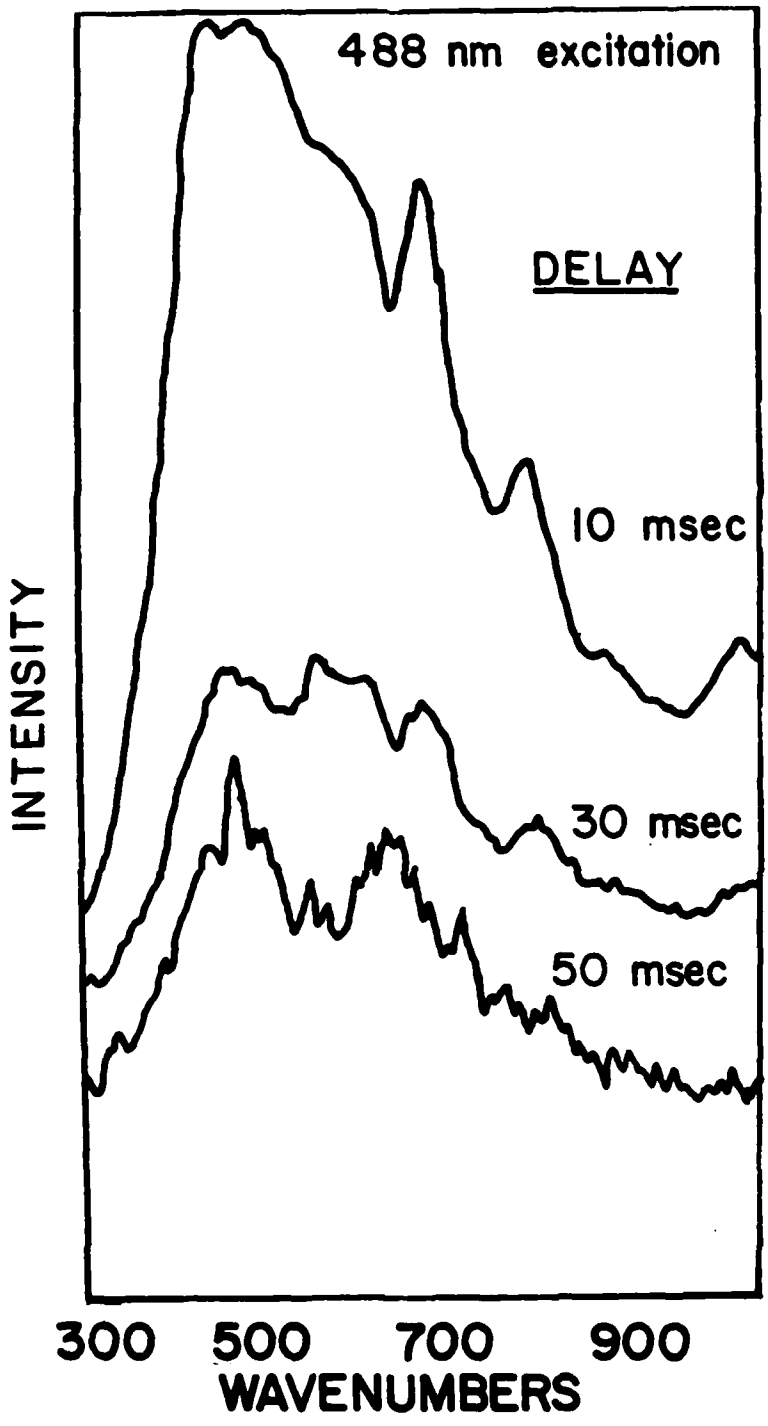

Figure 16. Time resolved raman spectra of a rutile coating subjected to a high energy laser damage pulse showing reversible transformation to an anatase-like phase. Spectra were acquired under CW Ar+ excitation on a millisecond time scale.

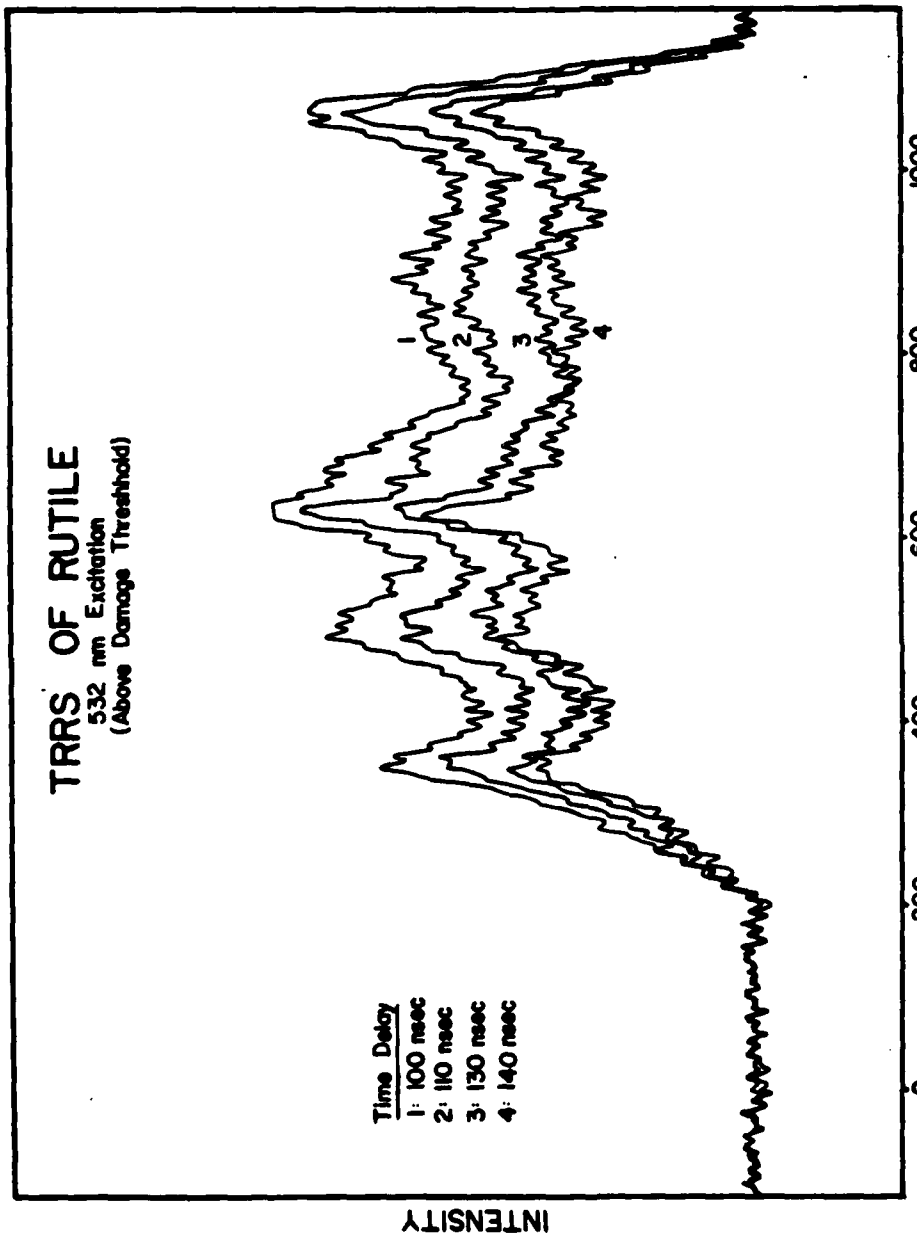

Figure 17. Time resolved raman spectra of a rutile coating subjected to a single high energy laser pulse acquired under 532 nm Nd:YAG excitation. Vibrational lines characteristic of the anatase lines are seen at short times following the damage pulse.

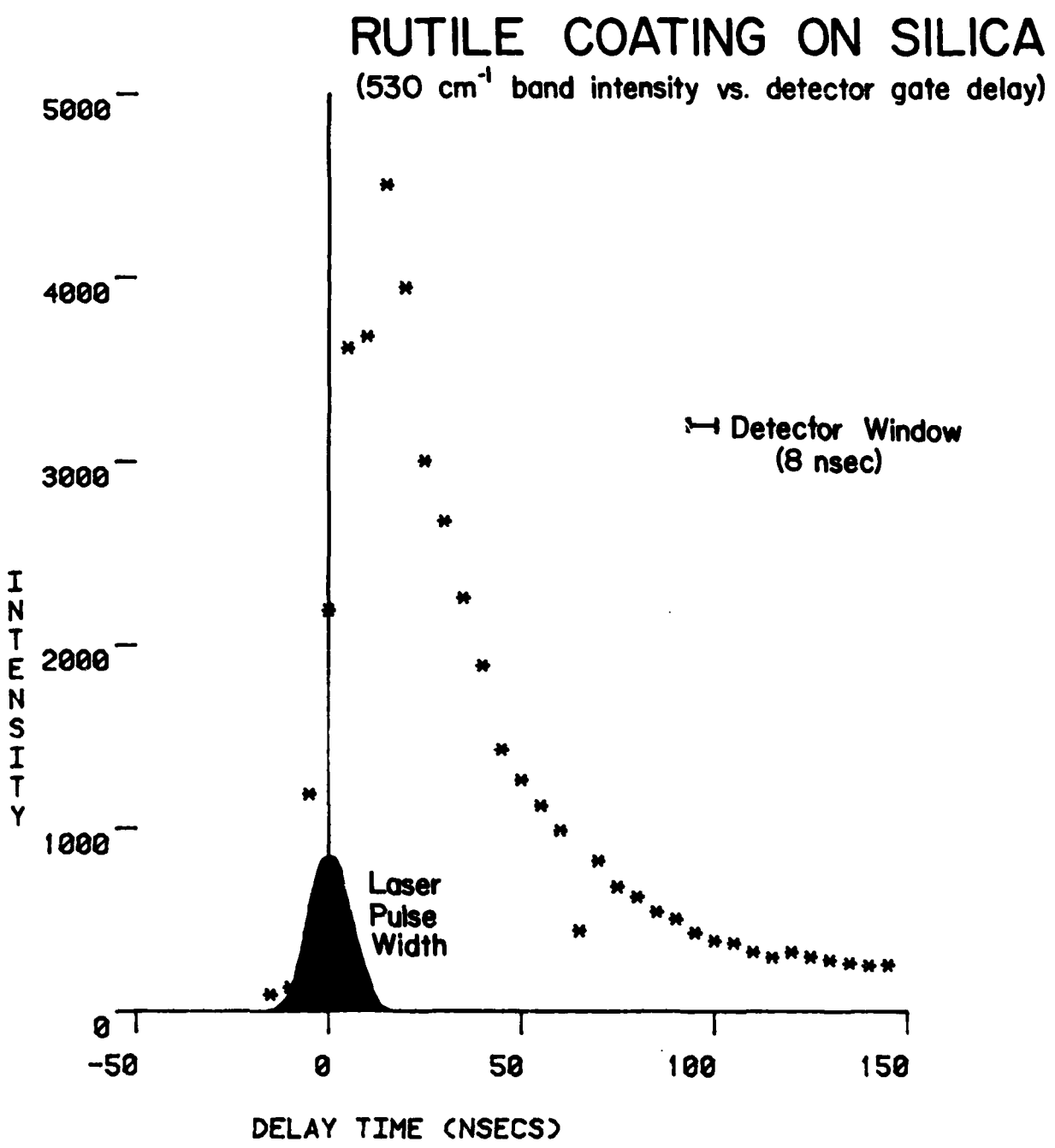

Figure 18. Intensity variation of the 530 cm^{-1} anatase-like band in a rutile coating during laser induced damage (532 nm) as a function of detector delay time.

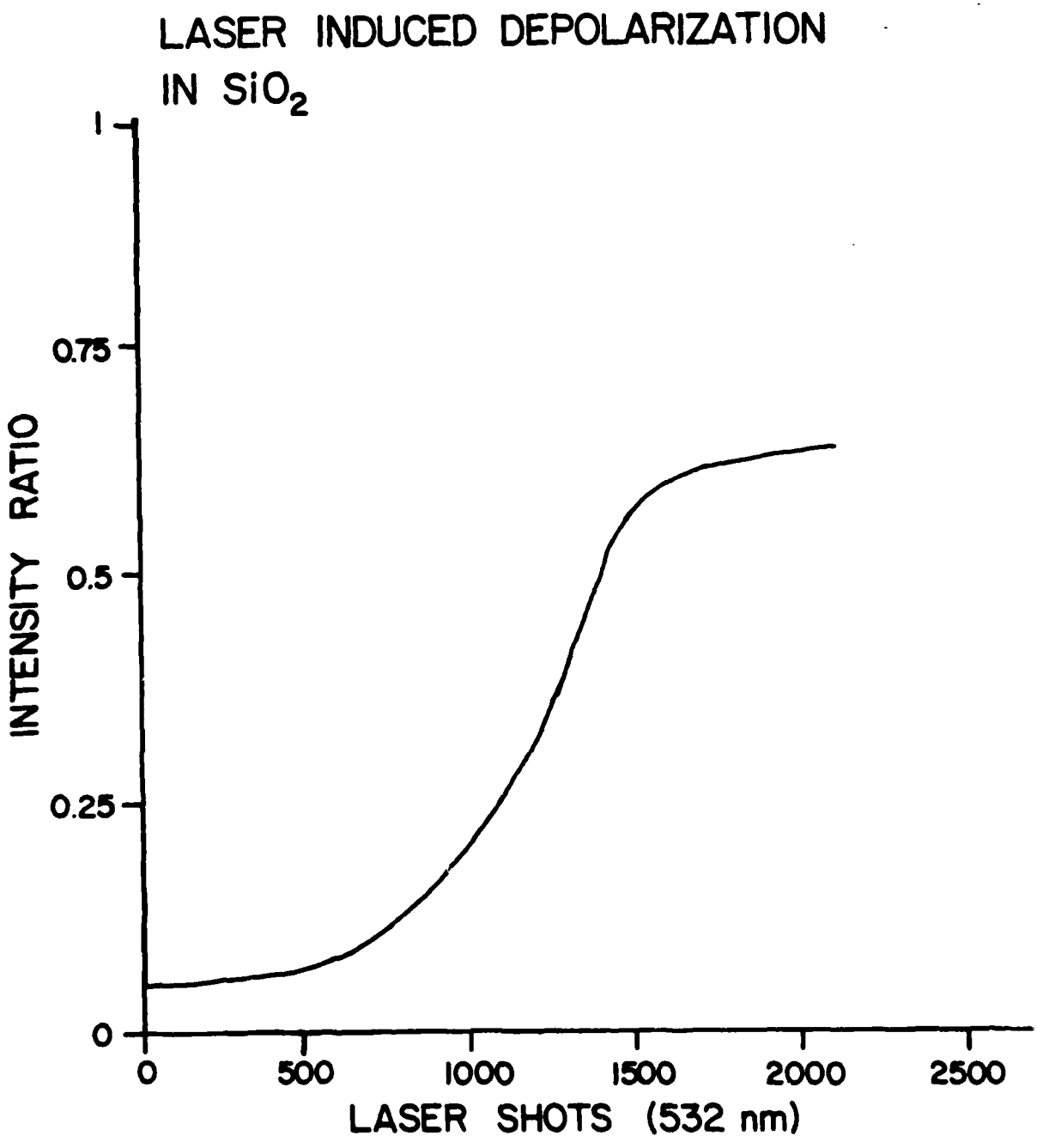

Figure 19. Induced polarization changes in a laser damaged SiO_2 glass substrate as a function of number of pulses. The intensity ratio refers to transmitted laser light through crossed polaroid filters relative to the parallel filter orientation.

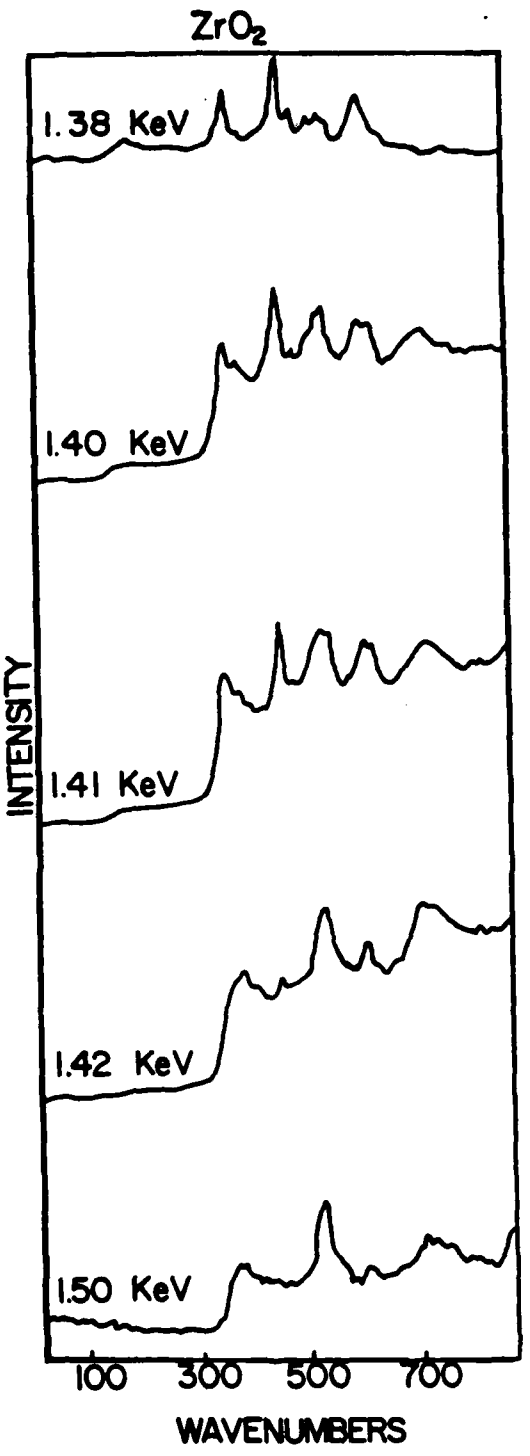

Figure 20. Raman spectra of single layer ZrO_2 on a metal substrate as a function of laser pulse energy. (The voltages refer to laser power supply settings and are proportional to laser output power.)

REFERENCES

1. Samara, G.A., and Peercy, P.S., "Pressure and Temperature Dependence of the Static Dielectric Constants and Raman Spectra of TiO_2 (Rutile)," Phys Rev. B. 7: pp. 1131-1148, 1973.

2. Nicol, M., and Fong, M.Y., "Raman Spectrum and Polymorphism of Titanium Dioxide at High Pressures," J. Chem. Phys. 54 (7): pp. 3167-3170, 1971.

3. Pawlewicz, W.T., Exarhos, G.J., and Conaway, W.E., "Structural Characterization of TiO_2 Optical Coatings by Raman Spectroscopy," Applied Optics 22 (12), pp. 1837-1840, 1983.

4. Newmanick, R.M., Connell, G.A.N., Hays, T.M., and Street, R.A., "Thermally Induced Effects in Evaporated Chalcogenide Films," Phys Rev. B 18, pp. 6900-6914, 1978.

5. Newmanick, R.J., Tsai, C.C., and Connell, G.N., "Interference-enhanced Raman Scattering of Very Thin Titanium and Titanium Oxide Films," Phys Rev Lett, 44: pp. 273-276, 1980.

6. Exarhos, G.J., and Pawlewicz, W.T., "Raman Characterization of All-dielectric Multilayer SiO_2/TiO_2 Optical Coatings," Applied Optics 23 (12): 1986-1988, 1984.

7. Exarhos, G.J., "Substrate Signal Suppression Ion Raman Spectra of Sputter Deposited TiO_2 Films," J. Chem. Phys., 81 (10), 000, 1984.

8. Parkes, G.D., Mellor's Modern Inorganic Chemistry, Revised Edition London; Longrans Publishing., p. 803, 1961.

9. Pawlewicz, W.T., Martin, P.M., Hays, D.D., and Mann, I.B. Recent developments in reactively sputtered optical thin films; Seddon, R.I., Ed. Proceedings of the SPIE Conference on Optical Thin Films, 1982 Jan, 26-27, Los Angeles, CA. Proc Soc Photo-Opt Instrument, Eng, 325, pp. 105-116, 1982.

10. Pawlewicz, W.T., Hays, D.C., and Martin, P.M., "High-band-gap Oxide Optical Coatings for 0.25 and 1.06 Micron Fusion Lasers," Thin Solid Films, 73, pp. 169-175, 1980.

11. Capwell, R.J., Spagnolo, K., and DeSesa, M.A., "A Rapid Determination of Low Concentrations of Anatase in Rutile TiO_2 Pigments by Raman Spectroscopy," Appl Spectrosco, 26: pp. 537-539, 1972.

12. Beattrie, I.R., and Gilson, T.R., "Single Crystal Laser Raman Spectroscopy, Proc. R. Soc. London Sec. A., 307: pp. 407-427, 1968.

13. Ohsaka, T., Yamaoka, S., and Shimomura, O., "Effect of Hydrostatic Pressure on the Raman Spectrum of Anatase (TiO_2)," Solid State Communications, Vol 30: pp. 345-347, 1979.

REFERENCES (Continued)

14. Royce, G.A., and Kay, R.B., "Multiphoton Interaction in Rutile," Applied Optics, 23 (12): pp. 1975-1979, 1984.

15. Figgis, B.N., Introduction to Ligand Fields, New York, Interscience Publishers, p. 193, 1966.

16. Munnix, S., and Schmeitz, M., "Surface Electronic Structure of Rutile-type Semiconductors, SnO_2 (110) and TiO_2 (110)," Surface Science 126, pp. 20-24, 1983.

17. Rosseau, D.L., and Williams, P.F., "Resonance Raman Scattering of Light from a Diatomic Molecule," J. Chem. Phys. 64 (9), pp. 3519-3537, 1976.

END

FILMED

12-85

DTIC